Chinese Journal of
POLYMER SCIENCE

RESEARCH ARTICLE

https://doi.org/10.1007/s10118-023-2937-z
Chinese J. Polym. Sci. **2023**, *41*, 824–831

3-Methylcyclohexanone Processed n-Channel Organic Thin-Film Transistors Based on a Conjugated Polymer Synthesized by Direct Arylation Polycondensation

Dong-Sheng Yan[a], Xu-Wen Zhang[a], Zhong-Li Wang[b*], Chen-Hui Xu[a], Yi-Bo Shi[a], Yun-Feng Deng[a], Yang Han[a], and Yan-Hou Geng[a,c*]

[a] *School of Materials Science and Engineering and Tianjin Key Laboratory of Molecular Optoelectronic Science, Tianjin University, and Collaborative Innovation Center of Chemical Science and Engineering (Tianjin), Tianjin 300072, China*
[b] *State Key Laboratory of Separation Membranes and Membrane Processes, Tianjin Key Laboratory of Advanced Fibers and Energy Storage, School of Material Science and Engineering, Tiangong University, Tianjin 300387, China*
[c] *Joint School of National University of Singapore and Tianjin University, International Campus of Tianjin University, Fuzhou 350207, China*

Electronic Supplementary Information

Abstract The solubility of a direct arylation polycondensation (DArP) synthesized conjugated polymer, *i.e.*, poly(3,6-bis(furan-2-yl)-2,5-bis(4-tetradecyloctadecyl)-pyrrolo[3,4-*c*]pyrrole-1,4(2*H*,5*H*)-dione-*alt*-1,2-bis(3,4-difluorothien-2-yl)ethene) (PFuDPP-4FTVT), in various organic solvents was studied. The polymer is soluble in 3-methylcyclohexanone (3-MC), a green solvent from peppermint oil, besides other solvents such as anisole, cyclopentyl methyl ether (CPME) and *o*-dichlorobenzene (*o*-DCB), *etc*. Based on the Hansen solubility parameters (HSP) analysis, 3-MC is identified as a "marginal solvent" of PFuDPP-4FTVT. The morphology of the spin-coated films with 3-MC as the solvent strongly correlated with the solution preparation conditions. With a 3-MC solution aged for 3 h at 70 °C, n-channel organic thin-film transistors (OTFTs) with electron mobility (μ_e) above 1 $cm^2 \cdot V^{-1} \cdot s^{-1}$ and current on/off ratio (I_{on}/I_{off}) higher than 10^5 were fabricated by spin-coating. This is the first report on high mobility conjugated polymers for OTFTs processible with naturally occurred green solvent.

Keywords Conjugated polymers; Organic thin-film transistors; Electron mobility; Green solvent; Direct arylation polycondensation

Citation: Yan, D. S.; Zhang, X. W.; Wang, Z. L.; Xu, C. H.; Shi, Y. B.; Deng, Y. F.; Han, Y.; Geng, Y. H. 3-Methylcyclohexanone processed n-channel organic thin-film transistors based on a conjugated polymer synthesized by direct arylation polycondensation. *Chinese J. Polym. Sci.* **2023**, *41*, 824–831.

INTRODUCTION

Conjugated polymers (CPs) have received tremendous research interest for their applications in optoelectronics such as organic thin-film transistors (OTFTs), organic photovoltaics (OPVs), and organic light-emitting diodes (OLEDs) due to their light weight, mechanical flexibility and large area solution processibility.[1] Donor-acceptor (D-A) CPs are one class of the most important high mobility CPs to date, and the mobility of OTFTs based on D-A CPs has exceeded 10 $cm^2 \cdot V^{-1} \cdot s^{-1}$.[2–4] Of D-A CPs for high performance OTFTs, those with diketopyrrolopyrrole (DPP) as electron-deficient or acceptor (A) unit are most studied in recent years.[5–14] For example, Kim *et al*. synthesized a copolymer of DPP and (*E*)-1,2-di(selenophen-2-yl)ethene (SVS), which exhibited a hole mobility up to 12.04 $cm^2 \cdot V^{-1} \cdot s^{-1}$ in spin-coated OTFT devices from chloroform.[9] Zhang *et al*. introduced urea groups in the side chains of DPP-tetrathiophene copolymers to enhance the packing order in films, and the resultant polymers exhibited field-effect hole mobility up to 13.1 $cm^2 \cdot V^{-1} \cdot s^{-1}$ with chloroform as processing solvent.[10] Recently, we also reported a DPP-based CP named as TDPP-Se. *Via* optimizing molecular weight, bar-coated OTFTs of the polymer with *o*-dichlorobenzene (*o*-DCB) as solvent showed a remarkably high hole mobility of 13.8 $cm^2 \cdot V^{-1} \cdot s^{-1}$.[11]

However, most of the high mobility D-A CPs reported so far possess poor solubility in non-chlorinated solvents due to strong intermolecular interaction, and thereby their OTFTs have to be fabricated with halogenated solvents such as chloroform, chlorobenzene and *o*-DCB.[9,11,14] It is well-known that halogenated solvents are highly toxic and harmful to the environment.[15] Therefore, it is crucial to develop high mobility CPs readily soluble in environmentally more benign solvents to meet the needs of future applications.[16,17] Several strategies have been developed to enhance the solubility of DPP-based CPs in non-halogenated solvents, including lowering regioregularity, increasing side chain density, using long

* Corresponding authors, E-mail: zhongliwang@tiangong.edu.cn (Z.L.W.)
E-mail: yanhou.geng@tju.edu.cn (Y.H.G.)

Special Issue: In Memory of Professor Fosong Wang
Received November 21, 2022; Accepted December 23, 2022; Published online February 21, 2023

siloxane side chain and so on.[18–25] As a result, OTFTs with moderate to high mobility were fabricated with toluene, tetralin, tetrahydrofuran (THF) and hexane.

According to CHEM21 and Sanofi's solvent selection guides, organic solvents are classified as three main categories: hazardous or highly hazardous, problematic and recommended.[26–28] Almost all halogenated solvents are ranked as hazardous or highly hazardous. Toluene and tetralin are non-halogenated aromatic solvents that are considered to be environmentally more benign than halogenated counterparts. However, according to aforementioned solvent selection guides, they are classified as problematic and hazardous, respectively. THF and hexane are non-halogenated and non-aromatic solvents. However, they are still not the recommended solvents. Especially, hexane is ranked as a hazardous solvent due to its high volatility and toxicity.[29] Recently, we and others found that D-A CPs comprising furan-flanked DPP moieties showed good solubility in some non-chlorinated solvents such as toluene, *o*-xylene and anisole.[23,30–33] We also fabricated OTFTs with mobility >1 $cm^2 \cdot V^{-1} \cdot s^{-1}$ by using anisole as the processing solvent, a recommended solvent according to the solvent selection guides.[23,33] However, anisole is still an aromatic solvent which may take a risk because benzene is a very toxic chemical during metabolism in human body.[34,35]

As a non-halogenated and non-aromatic solvent, 3-methylcyclohexanone (3-MC) is ranked as a recommended solvent according to solvent selection guides.[26–28] Furthermore, 3-MC is a natural chemical from peppermint oil that can be used as a food additive.[36,37] These features qualify 3-MC a real green solvent. Recently, Park *et al.* fabricated CP charge transport layer using 3-MC as the solvent for high-performance perovskite solar cells.[38] However, high mobility CPs processible with 3-MC is not reported yet. In the current paper, we select a direct arylation polycondensation (DArP) synthesized CP based on furan-flanked DPP, *i.e.*, poly(3,6-bis(furan-2-yl)-2,5-bis(4-tetradecyloctadecyl)-pyrrolo[3,4-*c*]pyrrole-1,4(2*H*,5*H*)-dione-*alt*-1,2-bis(3,4-difluorothien-2-yl)ethene) (PFuDPP-4FTVT), reported previously by us,[33] and its solubility in various organic solvents was investigated. We found that the polymer present moderate solubility in 3-MC. With this "marginal solvent", n-channel OTFTs with electron mobility (μ_e) above 1 $cm^2 \cdot V^{-1} \cdot s^{-1}$ were successfully prepared by spin-coating *via* optimizing solution preparation conditions. To the best of our knowledge, this is the first report on CP-based high mobility OTFTs processed with natural green solvent.

EXPERIMENTAL

Experimental details are outlined in the electronic supplementary information (ESI).

RESULTS AND DISCUSSION

Solubility of the Polymer

The structure of PFuDPP-4FTVT is shown in Fig. 1. The polymer was synthesized *via* DArP as reported previously. Its number-average molecular weight (M_n) and polydispersity index ($Đ$) of the polymer are 37.2 kDa and 2.1, respectively.[33]

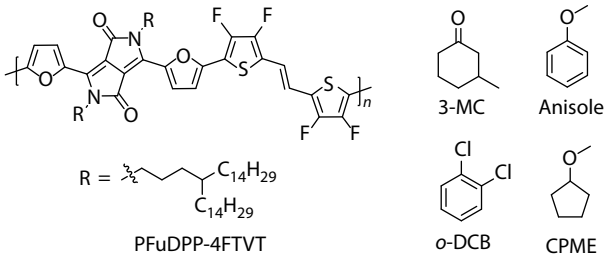

Fig. 1 Chemical structures of PFuDPP-4FTVT and selected solvents 3-MC, anisole, *o*-DCB and CPME.

The solubility of the polymer in different organic solvents was investigated at 70 °C (Table S1 in ESI). Among twenty-five solvents tested, eleven solvents could dissolve the polymer at a concentration of 3 $mg \cdot mL^{-1}$. Besides *o*-DCB, *o*-xylene and anisole reported previously, the polymer also shows good solubility in other eight solvents, including cyclopentyl methyl ether (CPME), toluene, 2-methyltetrahydrofuran, chloroform, chlorobenzene, 3-methylcyclohexanone (3-MC) and tetralin.

It is well known that the solvent has a profound effect on the film morphology and microstructures, and thereby OTFT device performance of CPs. Hansen solubility parameter (HSP) is a tool to study polymer-solvent interaction and has recently been used to correlate solvent, film morphology and device performance of various organic or polymeric semiconductors.[39–44] Therefore, HSPs of PFuDPP-4FTVT were determined by fitting the solubility test results of the polymer in twenty-five solvents (Table S1 in ESI) with HSPiP software following reference method.[45] As shown in Fig. 2, the coordinates of the center of the blue sphere correspond to the HSPs of PFuDPP-4FTVT with δ_D=18.12 $MPa^{0.5}$, δ_P=4.18 $MPa^{0.5}$ and δ_H=2.78 $MPa^{0.5}$, respectively. Herein, δ_D, δ_P and δ_H denote the dispersive solubility parameter, the polar solubility parameter, and the H-bonding solubility parameter, respectively. All "good solvents" are inside the HSP sphere and all "bad solvents" are outside the HSP sphere. The radius (R_0) of the blue sphere, equal to 4.20 $MPa^{0.5}$, defines the solubility limitation of PFuDPP-4FTVT. The HSP distance between the polymer and the solvent, called R_a, is the measure of how alike they are, and can be described as Eq. (1):

$$R_a^2 = 4(\delta_{D1} - \delta_{D2})^2 + (\delta_{P1} - \delta_{P2})^2 + (\delta_{H1} - \delta_{H2})^2 \quad (1)$$

In principle, the closer the coordinates of the solvent to the sphere center are, the stronger the relative affinity between the polymer and the solvent, and thereby higher solubility of the polymer in that solvent. The ability of the solvent to dissolve the polymer can be quantified as relative energy difference (RED) between the polymer and the solvent, which is expressed by Eq. (2):

$$\mathrm{RED} = \frac{R_a}{R_0} \quad (2)$$

According to the RED values summarized in parentheses on the right side in Fig. 2 and Table S1 in ESI, the twenty-five solvents can be classified as "good solvent" (with RED less than 1), "marginal solvent" (RED close to 1) and "poor solvent" (RED larger than 1). Four representative solvents 3-MC, anisole, *o*-DCB and cyclopentyl methyl ether (CPME) were selected to further study the solubility of the polymer. These four solvents can be classified as recommended (3-MC and an-

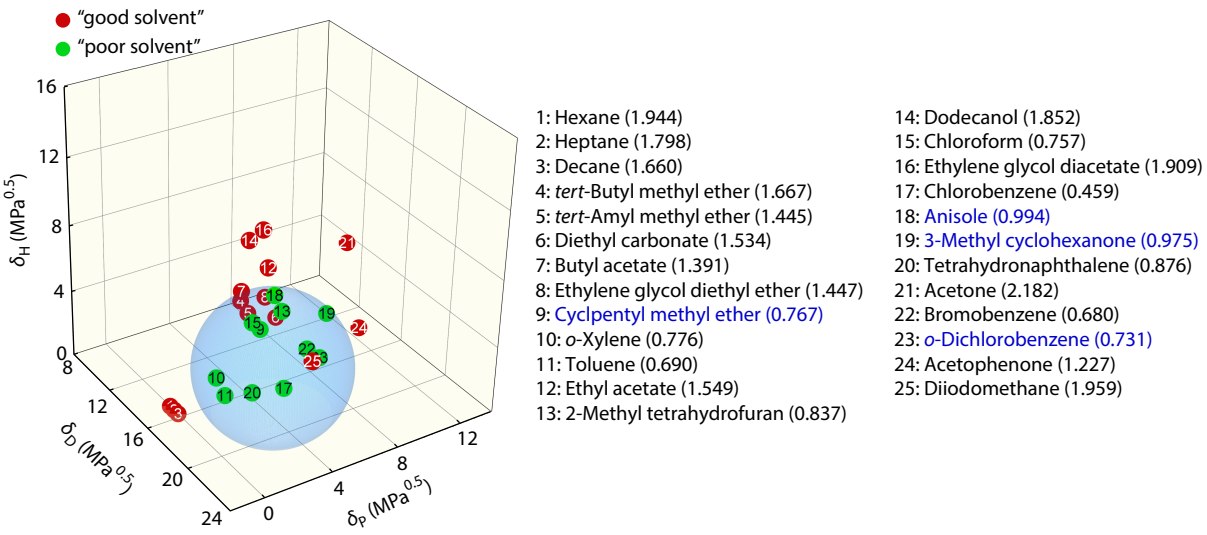

Fig. 2 Hansen solubility parameters of PFuDPP-4FTVT. Blue sphere centered at (18.12, 4.18, 2.78) MPa$^{0.5}$ with radius R_0=4.20 MPa$^{0.5}$ represents the soluble sphere of PFuDPP-4FTVT. The solvents tested are listed in right column, in which the numbers in parentheses denote relative energy difference (RED) values.

isole), problematic (CPME) and hazardous (*o*-DCB) according to solvent selection guides.[26] 3-MC and anisole, with RED values close to 1, are two "marginal solvents", while *o*-DCB and CPME are two good solvents with RED values obviously below 1. The solubility of PFuDPP-4FTVT in the four solvents at 70 °C was measured as 17.9 mg·mL^{-1} for 3-MC, 12.0 mg·mL^{-1} for anisole, 158.6 mg·mL^{-1} for *o*-DCB and 49.7 mg·mL^{-1} for CPME. The solubilities of the polymer in two "marginal solvents" are much lower than those in other two good solvents, consistent with above HSP analysis. The solubility of the polymer in *o*-DCB is much larger than that in CPME, although the RED values of these two solvents are very close. It is suggested that the contribution of δ_D to the cohesion energy density is greater than that of δ_P and δ_H.[40] This inconsistence might be attributed to the closer δ_D values between *o*-DCB and the polymer (19.2 MPa$^{0.5}$ versus 18.12 MPa$^{0.5}$).

The UV-Vis-NIR absorption spectra of the polymers in four different solvents, *i.e.*, 3-MC, anisole, *o*-DCB and CMPE, were recorded. As shown in Fig. 3(a), the spectra in four solvents all have a similar shape, with a weak absorption band centered at ~450 nm ascribed to the π-π^* transition and a strong absorption band at 600–900 nm originated from the intramolecular charge transfer (ICT). Absorption maxima were at 798, 798, 795 and 789 nm in 3-MC, anisole, *o*-DCB and CMPE, respectively. Pronounced vibronic peaks in the ICT band presents along with $A_{0\text{-}0}/A_{0\text{-}1}$ ratios >1.5, indicative of the strong aggregation of the polymer in all four solvents.[46,47]

To ascertain the strong aggregation of PFuDPP-4FTVT in solution, its temperature-dependent UV-Vis-NIR absorption spectra in above four solvents were recorded with the temperature no higher than 100 °C, the highest temperature used for OTFT fabrication. As shown in Fig. 3(b) and Fig. S1 in ESI, the 0-0 peak was obviously blue-shifted along with reduced $A_{0\text{-}0}/A_{0\text{-}1}$ as the solution temperature was enhanced, indicating partially disaggregation of the polymer chains. The blue shift (>20 nm) and reduction of 0-0 peak in *o*-DCB are the largest (Fig. 3c and Fig. S1 in ESI), implying the strongest disaggregation of the polymer upon heating in this solvent. This phenomenon is consistent with the highest solubility of the polymer in *o*-DCB. The degree of disaggregation of the polymer in CPME looks similar to that in 3-MC and anisole (Fig. 3c), although the solubility of the polymer in CPME is much larger. Note that CPME has the lowest boiling point (106 °C) among all four solvents, and the absorption spectrum at 100 °C was not measured.

The absorption spectra upon cooling from high temperature (90 °C for CPME solution and 100 °C for other three solutions) were also measured (Fig. S2 in ESI). In anisole, *o*-DCB and CPME, the spectra at same temperature in heating and cooling processes were almost overlapped, indicating the very fast re-organization or re-aggregation of the polymer chains upon cooling in these solvents. However, in 3-MC, the spectra in cooling process always showed a blue shift along with lower $A_{0\text{-}0}/A_{0\text{-}1}$ compared to the spectra measured at heating course. This means the re-organization of the polymer chains in 3-MC was relatively slow upon cooling (Fig. S1 in ESI).

OTFTs Performance

Top gate/bottom contact (TGBC) OTFTs were fabricated *via* spin-coating with 3-MC as the solvent. The semiconductor layer was spin-coated and thermally annealed at 200 °C for 10 min prior to the deposition of PMMA dielectric layer and gate electrode. An ultra-thin polyethylenimine ethoxylated (PEIE) layer was inserted between the gold source/drain electrodes and the polymer layer, allowing the efficient injection of electrons.[48] Device fabrication details are depicted in ESI. Considering the slow re-organization of the polymer in 3-MC, the polymer solutions were aged for 3 h at the given temperature prior to spin-coating. Three solution temperatures, 50, 70 and 100 °C, respectively, were used to explore the influence of solution temperature on device performance. All the devices exhibited typical n-channel operation behaviour. As shown in Fig. 4, with the devices fabricated at the solution

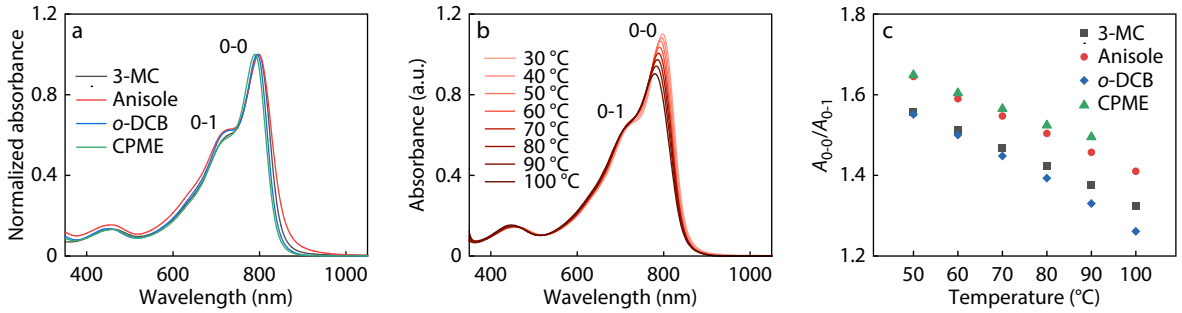

Fig. 3 (a) Solution UV-Vis-NIR absorption spectra of PFuDPP-4FTVT (1×10^{-5} mol·L^{-1}) in four different solvents; (b) Temperature-dependent solution UV-Vis-NIR absorption spectra of PFuDPP-4FTVT (1×10^{-5} mol·L^{-1}) in 3-MC upon heating; (c) $A_{0\text{-}0}/A_{0\text{-}1}$ at different temperatures in four different solvents.

temperature of 70 °C as example, near-ideal transfer and output curves along with the diminished dependence of μ_e on threshold voltage (V_T) were observed. This indicates that the extracted mobility values are reliable. The performance of the devices fabricated from 3-MC was obviously influenced by solution temperature. As shown in Table 1, the devices show the average electron mobility in saturation regime ($\mu_{e,sat}^{ave}$) of 0.60, 1.08 and 0.76 cm^2·V^{-1}·s^{-1} with the solution temperatures of 50, 70 and 100 °C, respectively. The μ_e values extracted form linear regime were very close to those extracted form saturation regime, consistent with high mobility reliability factors. Other three solvents anisole, *o*-DCB and CPME were also used to fabricate the devices for comparison. The 70 °C aged solutions were also delivered the best device performance, with $\mu_{e,sat}^{ave}$ values of 1.49, 1.08 and 1.19 cm^2·V^{-1}·s^{-1} for the devices processed with anisole, *o*-DCB and CPME, respectively (Fig. S3 in ESI and Table 1). With anisole and *o*-DCB as the solvents, the devices fabricated with 70 and 100 °C solutions all showed $\mu_{e,sat}^{ave}$ above 1 cm^2·V^{-1}·s^{-1}. the device performance with CPME was not very sensitive to solution temperature. The $\mu_{e,sat}^{ave}$ close to 1 cm^2·V^{-1}·s^{-1} was also obtained with the solution temperature of 50 and 100 °C. Obviously, the OTFTs processed with 3-MC at 70 °C had comparable performance with those processed with other three solvents. This is the first report on CP-based high mobility OTFTs processed with natural green solvent.

The influence of solution aging time on device performance was also investigated at the solution temperature of 70 °C (Table S2 in ESI). The performance of 3-MC processed devices is noticeably influenced by the aging time. The $\mu_{e,sat}^{ave}$ values were 0.65, 0.75, 1.08 and 0.52 cm^2·V^{-1}·s^{-1} for the devices with 0, 1, 3 and 6 h solution aging, respectively. Aging is also important for anisole processed devices. Without solution aging, the $\mu_{e,sat}^{ave}$ of the devices processed from anisole was 0.90 cm^2·V^{-1}·s^{-1}, lower than the $\mu_{e,sat}^{ave}$ of the devices with 3 h aged solution. In contrast, the device mobility was weakly dependent on aging time when two good solvents (*o*-DCB and CPME) were used. Without aging, the devices also exhibited the $\mu_{e,sat}^{ave}$ of 1.11 and 0.92 cm^2·V^{-1}·s^{-1} for *o*-DCB and CPME, respectively.

Film Morphology and Microstructures

To understand the influence of the solvent and solution temperature on device performance, the film morphology and microstructures were studied by using atomic force microscopy

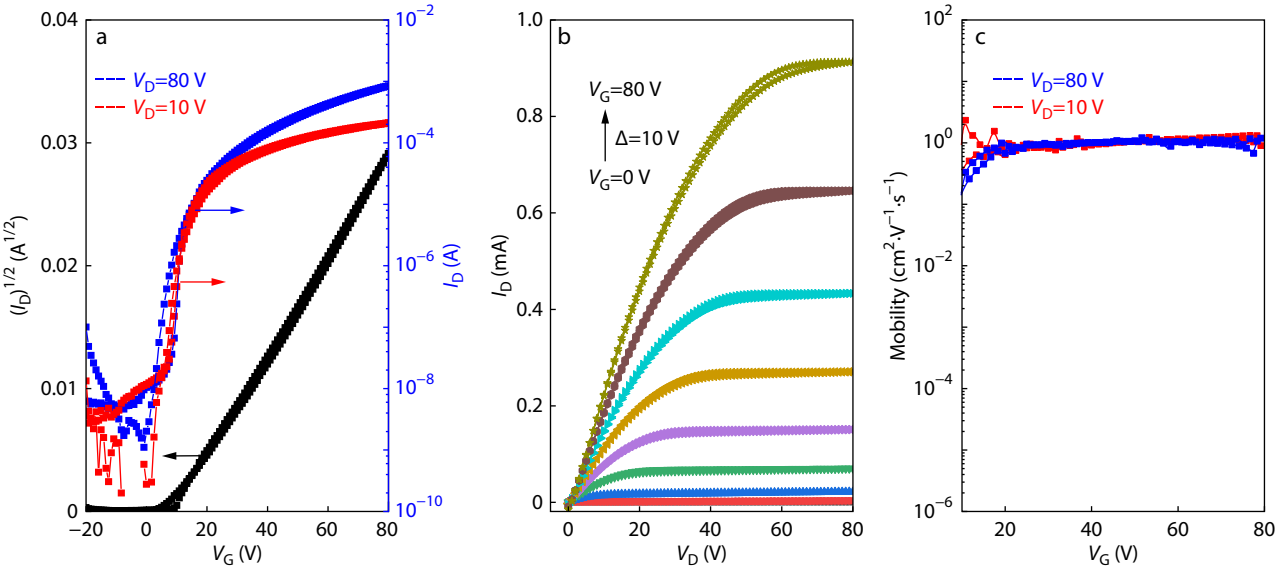

Fig. 4 (a) Typical transfer and (b) output characteristics and (c) saturation μ_e versus V_G of the OTFT devices based on PFuDPP-4FTVT spin-coated from 70 °C 3-MC solution with 3 h aging.

https://doi.org/10.1007/s10118-023-2937-z

Table 1 The performance data of spin-coated OTFT devices based on PFuDPP-4FTVT with different solvent and solution temperature. [a]

Solvent	Temperature [b] (°C)	$\mu_{e,sat}^{ave}$ ($\mu_{e,sat}^{max}$) [c] ($cm^2 \cdot V^{-1} \cdot s^{-1}$)	$\mu_{e,lin}^{ave}$ ($\mu_{e,lin}^{max}$) [d] ($cm^2 \cdot V^{-1} \cdot s^{-1}$)	V_T [e] (V)	I_{on}/I_{off} [f]	γ_{sat} (γ_{lin}) [g]
3-MC	50	0.76±0.08 (0.85)	0.73±0.10 (0.84)	9–11	10^5–10^6	75% (79%)
	70	1.08±0.03 (1.11)	1.03±0.05 (1.09)	8–10	10^6–10^7	80% (79%)
	100	0.60±0.01 (0.61)	0.60±0.02 (0.61)	10–12	10^6–10^7	78% (77%)
Anisole	50	0.64±0.21 (0.86)	0.63±0.22 (0.84)	14–17	10^6–10^7	68% (72%)
	70	1.49±0.19 (1.72)	1.48±0.27 (1.65)	7–9	10^4–10^5	80% (79%)
	100	1.23±0.07 (1.30)	1.20±0.07 (1.27)	10–12	10^4–10^5	72% (75%)
o-DCB	50	0.61±0.07 (0.68)	0.57±0.05 (0.62)	9–11	10^5–10^6	75% (70%)
	70	1.08±0.12 (1.22)	1.02±0.02 (1.04)	8–10	10^5–10^6	71% (70%)
	100	1.05±0.08 (1.12)	0.97±0.09 (1.03)	10–13	10^6–10^7	70% (71%)
CPME	50	0.94±0.02 (0.96)	0.91±0.03 (0.95)	6–8	10^5–10^6	76% (80%)
	70	1.19±0.05 (1.25)	1.01±0.10 (1.09)	5–9	10^5–10^6	82% (84%)
	100	0.95±0.11 (1.05)	0.88±0.11 (0.97)	6–8	10^6–10^7	82% (78%)

[a] All solutions were aged at given temperatures for 3 h prior to spin-coating; [b] Solution temperature; [c] Average and maximum (in parentheses) mobilities in saturation regime; [d] Average and maximum (in parentheses) mobilities in linear regime; [e] Threshold voltage; [f] Current on/off ratio; [g] Mobility reliability factor.

(AFM) and grazing incidence X-ray diffraction (GIXRD).[49–51] For all the thin films spin-coated with different solvents and solution temperatures, only the weak (100) diffraction peaks were observed in the out-of-plane direction and no any signals were detectible in the in-plane direction (Fig. S4 in ESI). In addition, paracrystalline disorder parameters (*g*)[52] of all the films were above 15% (Table S3 in ESI). All these indicate that PFuDPP-4FTVT is a near amorphous polymer.[36] Then, we postulate that the device performance of the polymer mainly correlates with film morphology and delicate inter-chain packing that is unable to detected so far. Fig. 5 shows the AFM topography images of the polymer films spin-coated from 3 h aged solutions at 50, 70 and 100 °C. For the films processed with 3-MC, the film morphology was very sensitive to the solution temperature and aging time. As shown in Figs. 5(a)–5(c), the film from the solution at 100 °C was uniform as indicated by small root-mean-square (RMS) roughness (0.57 nm) and featured short and finely fragmented fibrous morphology. With decreasing the aging temperature from 70 °C to 50 °C, the RMS roughness of the films was increased from 1.04 nm to 2.65 nm, respectively. For the film from the solution aged at 50 °C, the isolated large size aggregates distributed through all the film, which is detrimental to the charge transport in OTFTs. Although some of large size aggregates presented in the film

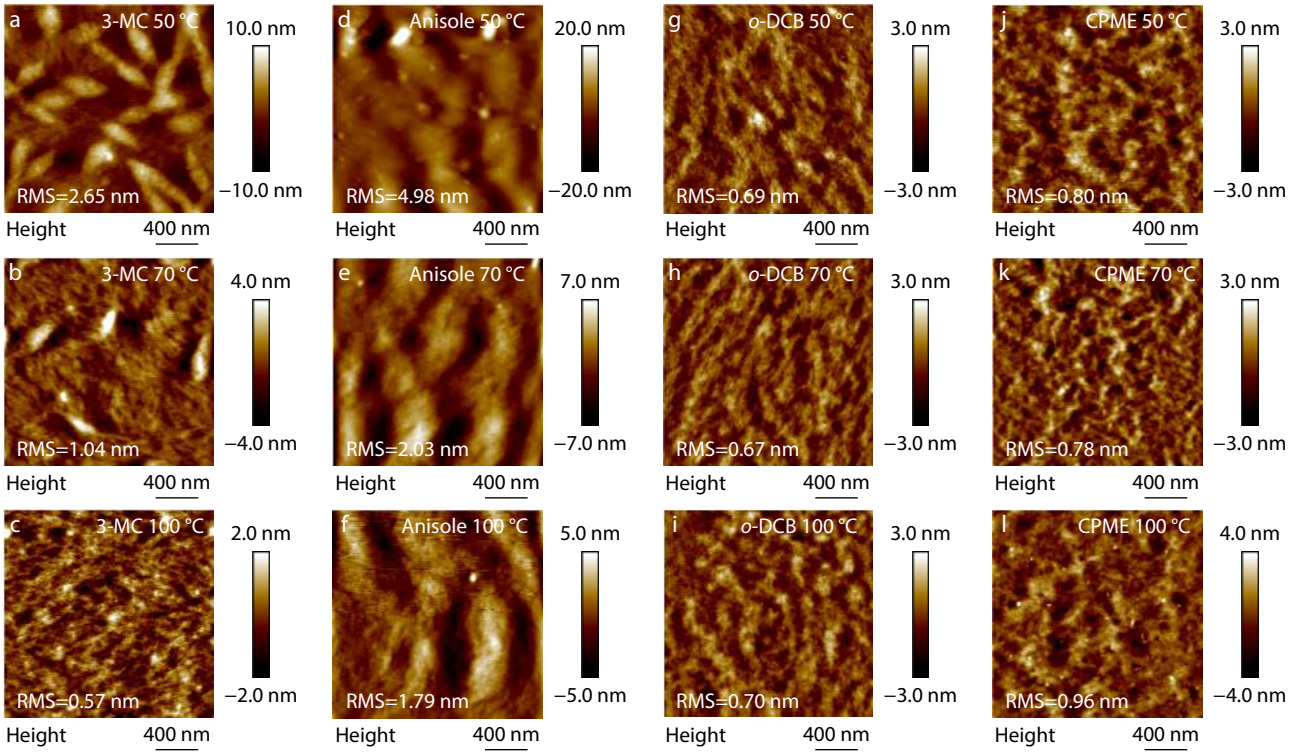

Fig. 5 AFM topography images (2 μm × 2 μm) of PFuDPP-4FTVT films spin-coated with different solvents and solution temperatures. The films were spin-coated from 3 mg·mL^{-1} solutions with 3 h aging. The substrates were at room temperature during spin-coating.

https://doi.org/10.1007/s10118-023-2937-z

from the solution at 70 °C, the film was featured as a more continuous fiber-like network structure on the surface, which is in favor to the efficient electron transport. This observation is consistent with above discussed device performance. The correlation between film morphology and device mobility was also observed when the aging time at 70 °C was varied from 0 h to 6 h. As shown in Fig. S5 (in ESI), the films from the solution without aging showed similar morphology to that prepared from the 3 h aged solution at 100 °C. With 1 and 3 h aging, the fibrous structures of the films became clearer. Further increasing aging time to 6 h led to more rough film with large size aggregates, like that presented in the film from 3 h aged solution at 50 °C. This evolution of the film morphology is also consistent with the device mobility variation trend as shown in Table S2 (in ESI). The dependence of film morphology on above solution preparation condition can be ascribed to the nature of "marginal solvent" of 3-MC. At 100 °C, polymer was well-dissolved. Uniform film featured with small RMS was formed due to the slow re-aggregation or re-organization rate of the polymer chains during the spin-coating process. At 50 °C, the polymer chains might strongly aggregate in solution, leading to the film with large size aggregates and then high surface roughness. At 70 °C, aging is necessary for the formation of aggregates, but long-time aging (such as 6 h) causes the formation of very large aggregates. The appropriate aggregation degree of the polymer in the 3 h aged solution at 70 °C led to the film with appropriate morphology.

Unlike the films spin-coated from 3-MC, the films processed from anisole at three different temperatures exhibited similar morphology with featureless inter-connected large domains, except for the very large RMS roughness of the film prepared from the 50 °C solution (Figs. 5d–5f). This may correlate with the fast re-organization of polymer chains in anisole upon cooling or solvent evaporation in spin-coating process. The morphology of the films prepared from two good solvents *o*-DCB and CPME is insensitive to solution temperature. All the films were very uniform with finely fragmented fibers and small RMS roughness regardless of solution temperature and aging time. The poorly inter-connected fiber-like nanostructures in the film spin-coated from the *o*-DCB solution at 50 °C were observed, consistent with the lower mobility of the devices fabricated at this temperature.

CONCLUSIONS

In conclusion, a DArP synthesized CP, PFuDPP-4FTVT, is soluble in a natural green solvent 3-MC, which is identified as a "marginal solvent" by HSP analysis. In addition, the reorganization or re-aggregation of the polymer is relatively slow upon cooling in this solvent. Thereby, the device performance strongly correlates with solution preparation conditions, including solution temperature and aging time. With the solution aged for 3 h at 70 °C, n-channel OTFTs with electron mobility above 1 $cm^2 \cdot V^{-1} \cdot s^{-1}$ were successfully fabricated. This work demonstrates that high mobility OTFTs processed with non-aromatic green solvent are attainable *via* appropriate design of CPs and optimization of device fabrication conditions.

NOTES

The authors declare no competing financial interest.

Electronic Supplementary Information

Electronic supplementary information (ESI) is available free of charge in the online version of this article at http://doi.org/10.1007/s10118-023-2937-z.

ACKNOWLEDGMENTS

This work was financially supported by the National Natural Science Foundation of China (Nos. 51933008 and 52121002) and the Fundamental Research Funds for the Central Universities.

REFERENCES

1 Huang, F.; Bo, Z. S.; Geng, Y. H.; Wang, X. H.; Wang, L. X.; Ma, Y. G.; Hou, J. H.; Hu, W. P.; Pei, J.; Dong, H. L.; Wang, S.; Li, Z.; Shuai, Z. G.; Li, Y. F.; Cao, Y. Study on optoelectronic polymers: an overview and outlook. *Acta Polymerica Sinica* (in Chinese) **2019**, *50*, 988–1046.
2 Kim, M.; Ryu, S. U.; Park, S. A.; Choi, K.; Kim, T.; Chung, D.; Park, T. Donor-acceptor-conjugated polymer for high-performance organic field-effect transistors: a progress report. *Adv. Funct. Mater.* **2019**, *30*, 1904545.
3 Zhou, Y.; Zhang, W.; Yu, G. Recent structural evolution of lactam- and imide-functionalized polymers applied in organic field-effect transistors and organic solar cells. *Chem. Sci.* **2021**, *12*, 6844–6878.
4 Chen, J.; Yang, J.; Guo, Y.; Liu, Y. Acceptor modulation strategies for improving the electron transport in high-performance organic field-effect transistors. *Adv. Mater.* **2022**, *34*, e2104325.
5 Liu, Q.; Bottle, S. E.; Sonar, P. Developments of diketopyrrolopyrrole-dye-based organic semiconductors for a wide range of applications in electronics. *Adv. Mater.* **2020**, *32*, e1903882.
6 Yang, Y.; Liu, Z.; Zhang, G.; Zhang, X.; Zhang, D. The effects of side chains on the charge mobilities and functionalities of semiconducting conjugated polymers beyond solubilities. *Adv. Mater.* **2019**, *31*, e1903104.
7 Nielsen, C. B.; Turbiez, M.; McCulloch, I. Recent advances in the development of semiconducting DPP-containing polymers for transistor applications. *Adv. Mater.* **2013**, *25*, 1859–1880.
8 Shen, T.; Li, W.; Zhao, Y.; Liu, Y.; Wang, Y. An all-C–H-activation strategy to rapidly synthesize high-mobility well-balanced ambipolar semiconducting polymers. *Matter* **2022**, *5*, 1953–1968.
9 Kang, I.; Yun, H. J.; Chung, D. S.; Kwon, S. K.; Kim, Y. H. Record high hole mobility in polymer semiconductors *via* side-chain engineering. *J. Am. Chem. Soc.* **2013**, *135*, 14896–14899.
10 Yao, J.; Yu, C.; Liu, Z.; Luo, H.; Yang, Y.; Zhang, G.; Zhang, D. Significant improvement of semiconducting performance of the diketopyrrolopyrrole-quaterthiophene conjugated polymer through side-chain engineering *via* hydrogen-bonding. *J. Am. Chem. Soc.* **2016**, *138*, 173–185.
11 Wang, Z.; Gao, M.; He, C.; Shi, W.; Deng, Y.; Han, Y.; Ye, L.; Geng, Y. Unraveling the molar mass dependence of shearing-induced aggregation structure of a high-mobility polymer semiconductor. *Adv. Mater.* **2022**, *34*, e2108255.
12 Zhang, A.; Xiao, C.; Wu, Y.; Li, C.; Ji, Y.; Li, L.; Hu, W.; Wang, Z.; Ma,

W.; Li, W. Effect of fluorination on molecular orientation of conjugated polymers in high performance field-effect transistors. *Macromolecules* **2016**, *49*, 6431–6438.
13 Back, J. Y.; Yu, H.; Song, I.; Kang, I.; Ahn, H.; Shin, T. J.; Kwon, S. K.; Oh, J. H.; Kim, Y. H. Investigation of structure-property relationships in diketopyrrolopyrrole-based polymer semiconductors *via* side-chain engineering. *Chem. Mater.* **2015**, *27*, 1732–1739.
14 Lv, S. Y.; Li, Q. Y.; Li, B. W.; Wang, J. Y.; Mu, Y. B.; Li, L.; Pei, J.; Wan, X. B. Thiazole-flanked thiazoloisoindigo as a monomer for balanced ambipolar polymeric field-effect transistors. *Chinese J. Polym. Sci.* **2022**, *40*, 1131–1140.
15 Capello, C.; Fischer, U.; Hungerbühler, K. What is a green solvent? A comprehensive framework for the environmental assessment of solvents. *Green Chem.* **2007**, *9*, 927–934.
16 Campana, F.; Kim, C.; Marrocchi, A.; Vaccaro, L. Green solvent-processed organic electronic devices. *J. Mater. Chem. C* **2020**, *8*, 15027–15047.
17 Ran, Y.; Guo, Y.; Liu, Y. Organostannane-free polycondensation and eco-friendly processing strategy for the design of semiconducting polymers in transistors. *Mater. Horiz.* **2020**, *7*, 1955–1970.
18 Choi, H. H.; Baek, J. Y.; Song, E.; Kang, B.; Cho, K.; Kwon, S.-K.; Kim, Y. H. A pseudo-regular alternating conjugated copolymer using an asymmetric monomer: a high-mobility organic transistor in nonchlorinated solvents. *Adv. Mater.* **2015**, *27*, 3626–3631.
19 Ji, Y.; Xiao, C.; Wang, Q.; Zhang, J.; Li, C.; Wu, Y.; Wei, Z.; Zhan, X.; Hu, W.; Wang, Z.; Janssen, R. A. J.; Li, W. Asymmetric diketopyrrolopyrrole conjugated polymers for field-effect transistors and polymer solar cells processed from a nonchlorinated solvent. *Adv. Mater.* **2016**, *28*, 943–950.
20 Yun, H. J.; Lee, G. B.; Chung, D. S.; Kim, Y. H.; Kwon, S. K. Novel diketopyrroloppyrrole random copolymers: high charge-carrier mobility from environmentally benign processing. *Adv. Mater.* **2014**, *26*, 6612–6616.
21 Ding, S.; Ni, Z.; Hu, M.; Qiu, G.; Li, J.; Ye, J.; Zhang, X.; Liu, F.; Dong, H.; Hu, W. An asymmetric furan/thieno[3,2-*b*]thiophene diketopyrrolopyrrole building block for annealing-free green-solvent processable organic thin-film transistors. *Macromol. Rapid Commun.* **2018**, *39*, e1800225.
22 Wang, Z.; Song, X.; Jiang, Y.; Zhang, J.; Yu, X.; Deng, Y.; Han, Y.; Hu, W.; Geng, Y. A simple structure conjugated polymer for high mobility organic thin film transistors processed from nonchlorinated solvent. *Adv. Sci.* **2019**, *6*, 1902412.
23 Wang, Z.; Shi, Y.; Deng, Y.; Han, Y.; Geng, Y. Toward high mobility green solvent-processable conjugated polymers: a systematic study on chalcogen effect in poly(diketopyrrolopyrrole-*alt*-terchalcogenophene)s. *Adv. Funct. Mater.* **2021**, *31*, 2104881.
24 Ding, Y.; Zhao, F.; Kim, S.; Wang, X.; Lu, H.; Zhang, G.; Cho, K.; Qiu, L. Azaisoindigo-based polymers with a linear hybrid siloxane-based side chain for high-performance semiconductors processable with nonchlorinated solvents. *ACS Appl. Mater. Interfaces* **2020**, *12*, 41832–41841.
25 Ding, Y.; Jiang, L.; Du, Y.; Kim, S.; Wang, X.; Lu, H.; Zhang, G.; Cho, K.; Qiu, L. Linear hybrid siloxane-based side chains for highly soluble isoindigo-based conjugated polymers. *Chem. Commun.* **2020**, *56*, 11867–11870.
26 Prat, D.; Wells, A.; Hayler, J.; Sneddon, H.; McElroy, C. R.; Abou-Shehada, S.; Dunn, P. J. CHEM21 selection guide of classical- and less classical-solvents. *Green Chem.* **2016**, *18*, 288–296.
27 Alder, C. M.; Hayler, J. D.; Henderson, R. K.; Redman, A. M.; Shukla, L.; Shuster, L. E.; Sneddon, H. F. Updating and further expanding GSK's solvent sustainability guide. *Green Chem.* **2016**, *18*, 3879–3890.
28 Prat, D.; Pardigon, O.; Flemming, H.-W.; Letestu, S.; Ducandas, V.; Isnard, P.; Guntrum, E.; Senac, T.; Ruisseau, S.; Cruciani, P.; Hosek, P. Sanofi's solvent selection guide: a step toward more sustainable processes. *Org. Process Res. Dev.* **2013**, *17*, 1517–1525.
29 Alfonsi, K.; Colberg, J.; Dunn, P. J.; Fevig, T.; Jennings, S.; Johnson, T. A.; Kleine, H. P.; Knight, C.; Nagy, M. A.; Perry, D. A.; Stefaniak, M. Green chemistry tools to influence a medicinal chemistry and research chemistry based organisation. *Green Chem.* **2008**, *10*, 31–36.
30 Chen, M. S.; Lee, O. P.; Niskala, J. R.; Yiu, A. T.; Tassone, C. J.; Schmidt, K.; Beaujuge, P. M.; Onishi, S. S.; Toney, M. F.; Zettl, A.; Fréchet, J. M. J. Enhanced solid-state order and field-effect hole mobility through control of nanoscale polymer aggregation. *J. Am. Chem. Soc.* **2013**, *135*, 19229–19236.
31 Sonar, P.; Chang, J.; Kim, J. H.; Ong, K. H.; Gann, E.; Manzhos, S.; Wu, J.; McNeill, C. R. High-mobility ambipolar organic thin-film transistor processed from a nonchlorinated solvent. *ACS Appl. Mater. Interfaces* **2016**, *8*, 24325–24330.
32 Lee, S. M.; Lee, H. R.; Han, A. R.; Lee, J.; Oh, J. H.; Yang, C. High-performance furan-containing conjugated polymer for environmentally benign solution processing. *ACS Appl. Mater. Interfaces* **2017**, *9*, 15652–15661.
33 Sui, Y.; Wang, Z.; Bai, J.; Shi, Y.; Zhang, X.; Deng, Y.; Han, Y.; Geng, Y. Diketopyrrolopyrrole-based conjugated polymers synthesized by direct arylation polycondensation for anisole-processed high mobility organic thin-film transistors. *J. Mater. Chem. C* **2022**, *10*, 2616–2622.
34 Li, C.; Misovich, M. V.; Pardo, M.; Fang, Z.; Laskin, A.; Chen, J.; Rudich, Y. Secondary organic aerosol formation from atmospheric reactions of anisole and associated health effects. *Chemosphere* **2022**, *308*, 136421.
35 Snyder, R.; Hedli, C. C. An overview of benzene metabolism. *Environ. Health Perspect* **1996**, *104*, 1165–1171.
36 Mohaddese M.; Nastaran K. Chemical composition and antimicrobial activity of peppermint (mentha piperita L.) essential oil. *Songklanakarin J. Sci. Technol.* **2014**, *36*, 83–87.
37 Newberne, P; Doull, J; Feron, V. J.; Goodman, J. I.; Munro, I. C.; Portoghese, P. S.; Waddell, W. J.; Wagner, B. M.; Weil, C. S.; Adams, T. B.; Hallagan, J. B. GRAS flavoring substances 19. *Food Technol.* **2000**, *54*, 66–84.
38 Lee, J.; Kim, G. W.; Kim, M.; Park, S. A.; Park, T. Nonaromatic green-solvent-processable, dopant-free, and lead-capturable hole transport polymers in perovskite solar cells with high efficiency. *Adv. Energy Mater.* **2020**, *10*, 1902662.
39 Machui, F.; Abbott, S.; Waller, D.; Koppe, M.; Brabec, C. J. Determination of Solubility Parameters for organic semiconductor formulations. *Macromol. Chem. Phys.* **2011**, *212*, 2159–2165.
40 Kim, N. K.; Shin, E. S.; Noh, Y. Y.; Kim, D. Y. A selection rule of solvent for highly aligned diketopyrrolopyrrole-based conjugated polymer film for high performance organic field-effect transistors. *Org. Electron.* **2018**, *55*, 6–14.
41 Dereje, M. M.; Ji, D.; Kang, S.H.; Yang, C.; Noh, Y. Y. Effect of pre-aggregation in conjugated polymer solution on performance of diketopyrrolopyrrole-based organic field-effect transistors. *Dyes Pigments* **2017**, *145*, 270–276.
42 Gaikwad, A. M.; Khan, Y.; Ostfeld, A. E.; Pandya, S.; Abraham, S.; Arias, A. C. Identifying orthogonal solvents for solution processed organic transistors. *Org. Electron.* **2016**, *30*, 18–29.
43 Li, H.; Liu, X.; Jin, T.; Zhao, K.; Zhang, Q.; He, C.; Yang, H.; Chen, Y.; Huang, J.; Yu, X.; Han, Y. Optimizing the intercrystallite connection of a donor-acceptor conjugated semiconductor polymer by controlling the crystallization rate *via* temperature. *Macromol. Rapid Commun.* **2022**, *43*, e2200084.
44 Zhao, K.; Zhang, Q.; Chen, L.; Zhang, T.; Han, Y. Nucleation and

growth of P(NDI2OD-T2) nanowires *via* side chain ordering and backbone planarization. *Macromolecules* **2021**, *54*, 2143–2154.
45 Hansen, C. M. in *Hansen Solubility Parameters: A User's Handbook*. CRC Press: Boca Raton, **2007**, p. 75.
46 Panzer, F.; Bassler, H.; Kohler, A. Temperature induced order-disorder transition in solutions of conjugated polymers probed by optical spectroscopy. *J. Phys. Chem. Lett.* **2017**, *8*, 114–125.
47 Schroeder, B. C.; Chiu, Y. C.; Gu, X.; Zhou, Y.; Xu, J.; Lopez, J.; Lu, C.; Toney, M. F.; Bao, Z. Non-conjugated flexible linkers in semiconducting polymers: a pathway to improved processability without compromising device performance. *Adv. Electron. Mater.* **2016**, *2*, 1600104.
48 Zhou, Y.; Fuentes-Hernandez, C.; Shim, J.; Meyer, J.; Giordano, A. J.; Li, H.; Winget, P.; Papadopoulos, T.; Cheun, H.; Kim, J.; Fenoll, M.; Dindar, A.; Haske, W.; Najafabadi, E.; Khan, T. M.; Sojoudi, H.; Barlow, S.; Graham, S.; Bredas, J. L.; Marder, S. R.; Kahn, A.; Kippelen, B. A universal method to produce low-work function electrodes for organic electronics. *Science* **2012**, *336*, 327–332.
49 Dong, H.; Jiang, S.; Jiang, L.; Liu, Y.; Li, H.; Hu, W.; Wang, E.; Yan, S.; Wei, Z.; Xu, W.; Gong, X. Nanowire crystals of a rigid rod conjugated polymer. *J. Am. Chem. Soc.* **2009**, *131*, 17315–17320.
50 Yao, Y.; Dong, H.; Liu, F.; Russell, T. P.; Hu, W. Approaching intra- and interchain charge transport of conjugated polymers facilely by topochemical polymerized single crystals. *Adv. Mater.* **2017**, *29*, 1701251.
51 Yao, Z. F.; Li, Q. Y.; Wu, H. T.; Ding, Y. F.; Wang, Z. Y.; Lu, Y.; Wang, J. Y.; Pei, J. Building crystal structures of conjugated polymers through X-ray diffraction and molecular modeling. *SmartMat* **2021**, *2*, 378–387.
52 Rivnay, J.; Noriega, R.; Kline, R. J.; Salleo, A.; Toney, M. F. Quantitative analysis of lattice disorder and crystallite size in organic semiconductor thin films. *Phys. Rev. B* **2011**, *84*, 045203.

https://doi.org/10.1007/s10118-023-2937-z